Change ΔS of the entropy in natural time under time reversal: Complexity measures upon change of scale

Sarlis, N.V. , Christopoulos, S-R. and Bemplidaki, M.M.

Original citation:
Sarlis, N.V. , Christopoulos, S-R. and Bemplidaki, M.M. (2015) Change ΔS of the entropy in natural time under time reversal: Complexity measures upon change of scale. EPL (Europhysics Letters), volume 109 (1). DOI: 10.1209/0295-5075/109/18002

http://dx.doi.org/10.1209/0295-5075/109/18002

European Physical Society

Change $\triangle S$ of the entropy in natural time under time reversal: Complexity measures upon change of scale.

N. V. Sarlis[1], S.-R. G. Christopoulos[1] and M. M. Bemplidaki[1]

[1] *Department of Solid State Physics and Solid Earth Physics Institute, Faculty of Physics, School of Science, National and Kapodistrian University of Athens, Panepistimiopolis, Zografos 157 84, Athens, Greece, EU*

PACS 87.10.-e – General theory and mathematical aspects
PACS 87.19.Hh – Cardiac dynamics
PACS 89.75.-k – Complex systems

Abstract –The entropy S in natural time as well as the entropy in natural time under time reversal S_- have already found useful applications in the physics of complex systems, e.g., in the analysis of electrocardiograms (ECGs). Here, we focus on the complexity measures Λ_l which result upon considering how the statistics of the time series $\Delta S\,[\equiv S - S_-]$ changes upon varying the scale l. These scale specific measures are ratios of the standard deviations $\sigma(\Delta S_l)$ and hence independent of the mean value and the standard deviation of the data. They focus on the different dynamics that appear on different scales. For this reason, they can be considered complementary to other standard measures of heart rate variability in ECG, like SDNN, as well as other complexity measures already defined in natural time. An application to the analysis of ECG -when solely using NN intervals- is presented: We show how Λ_l can be used to separate ECG of healthy individuals from those suffering from congestive heart failure and sudden cardiac death.

Introduction. – Natural time analysis [1–3] focuses in the sequential order of events occurring in a complex system. It extracts the maximum information possible from a given time series [4]. If we consider a series of N events in a complex system, the natural time attributed to the k-th event is given by $\chi_k = k/N$. For example, as shown in fig.1, in the case of an electrocardiogram (ECG) as events we may consider the heartbeats. In natural time analysis, χ_k is complemented by a quantity Q_k which is proportional to the energy emitted during the k-th event. Further analysis is made by studying the pair (χ_k, Q_k) and introducing the normalized energy $p_k = Q_k / \sum_{n=1}^{N} Q_n$. Since $p_k (k = 1, 2, \ldots N)$ sum up to unity, they can be considered as probabilities corresponding to χ_k. The entropy S in natural time is defined [1, 5, 6] by

$$S = \langle \chi \ln \chi \rangle - \langle \chi \rangle \ln \langle \chi \rangle, \tag{1}$$

where the brackets $\langle \ldots \rangle$ denote averages with respect to the distribution p_k, i.e., $\langle f(\chi) \rangle \equiv \sum_{k=1}^{N} f(\chi_k) p_k$. The entropy S is a dynamic entropy that exhibits [7] positivity, concavity and Lesche [8, 9] experimental stability. The entropy corresponding to the 'uniform' distribution, i.e., when $p_k = 1/N$ (e.g. see refs. [3,5,10,11]), is $S_u = \frac{\ln 2}{2} - \frac{1}{4} \approx 0.0966$. Moreover, upon considering time reversal $\mathcal{T}$, i.e., $\mathcal{T} p_k = p_{N-k+1}$ (see fig.1(d)), the value of S changes

to a value S_-:

$$S_- = \langle \chi \ln \chi \rangle_{\mathcal{T}} - \langle \chi \rangle_{\mathcal{T}} \ln \langle \chi \rangle_{\mathcal{T}}, \tag{2}$$

where $\langle f(\chi) \rangle_{\mathcal{T}} \equiv \sum_{k=1}^{N} f(\chi_k) p_{N-k+1}$. The physical meaning of the change of entropy $\Delta S \equiv S - S_-$ in natural time under time reversal has been studied [3, 12, 13] using the distributions $p(\chi;\epsilon) = 1+\epsilon(\chi-1/2)$ which replace p_k when considering a continuous variable $\chi \in (0,1]$ instead of χ_k. Small $\epsilon(<1)$, represents an increase ($\epsilon > 0$) or decrease ($\epsilon < 0$) of Q_k when k increases, thus reflecting the effect of small linear trends in Q_k. It can be shown [3, 12] that $\Delta S(\epsilon) = \left(\frac{6\ln 2-5}{36}\right)\epsilon + O(\epsilon^3)$, leading to the conclusion that a small increasing trend leads to negative ΔS and vice versa. The change of the entropy ΔS in natural time has found useful applications in the study [14] of the predictability of the Olami-Feder-Christensen dynamical model [15] for earthquakes, in atmospheric physics [16, 17], and in the analysis of ECG [3, 12, 18] to which we now turn.

Interestingly, physiological signals reflect both self-regulation to reduce variability and a high degree of complexity [19]. This complexity is of course reflected in the corresponding electric signals from ECG (e.g., see refs. [20,21]) or electroencephalography (EEG) [22]. The study of long range correlations in heart dynamics [23–27] has revealed a rich multifractality for healthy dynamics [19] which breaks down in illness [28–33]. For these reasons, scale-specific and scale-independent complexity measures have been employed [34] using well established methods of Statistical Physics, i.e., Detrended Fluctuation Analysis [24, 35, 36] and Wavelet Analysis (e.g., see ref. [28] and references therein). It has been shown [34] that scale-specific and scale-independent measures are uncorrelated and that the former (scale-specific) perform better as diagnostic tools whereas the latter (scale-independent) as prediction tools. Moreover, since physiological signals may contain both stochastic and deterministic components, the concept of entropy is also suitable for the study of ECG. For example, multiscale entropy has been applied [37] to Heart Period (HP) variability in ECG revealing the importance of different scale-specific complexity measures to separate healthy from pathologic groups. Additionally, the importance of time irreversibility has been highlighted in many studies [38–43]. More specifically in ref. [38], a multiscale time asymmetry index was proposed which is highest for a time series from young healthy subjects and decreases with aging or heart disease and in refs. [39, 40, 43] several complexity metrics under time reversal have been studied and applied in the HP variability in fetuses, adult healthy subjects and pathological patients under different experimental conditions. Some of the related metrics and methods, e.g. those defined in ref. [39], have been studied as a function of the time scales [41, 42]. Time irreversibility at a single time scale was specifically assessed [43] over HP variability in healthy and a pathological group of age-matched chronic heart failure patients. It was found [43] that the patients exhibit time irreversibility more often than in healthy controls and time irreversibility markers show circadian rhythmicity. Taking into account all the above studies, we provide below a multiscale entropy analysis in natural time, aiming to the distinction of three groups, i.e. healthy subjects, congestive heart failure (CHF) patients and sudden cardiac death (SCD) individuals.

Natural time entropy of eq.(1) has been also used in ECG. Complexity measures have been introduced [6, 44, 45] to quantify the variability of the natural entropy fluctuations upon changing either the (natural time window) length scale or shuffling the consecutive events randomly. In these studies, Q_k has been set equal to various duration intervals defined in an ECG , where the turning points are marked by the letters P, Q, R, S and T (fig.1), e.g., $Q_k = \mathrm{RR}_k$. Using a moving window of length l heartbeats sliding through the time series of L consecutive ECG intervals the entropy in natural time has been determined for each position $j = 1, 2, \ldots, L-l$ of the sliding window by considering $p_k = \mathrm{RR}_{j+k} / \sum_{k=1}^{l} \mathrm{RR}_{j+k}, k = 1, 2, \ldots, l$ and $\langle f(\chi) \rangle \equiv \sum_{k=1}^{l} f(\chi_k) p_k$ in eq.(1). Thus, a time series of S_l has been constructed [6] whose standard deviation δS_l was compared to the standard deviation $\delta S_{l,shuff}$ obtained by the same procedure when shuffling randomly the ECG intervals time series. The results showed that the ratios $\delta S_{l,shuff}/\delta S_l$ provide useful

information for the characterization of ECG. This study was later generalized [45] to include the effect of the change of scale l on δS_l by means of the complexity measure $\lambda_l = \delta S_l/\delta S_3$ revealing the importance of the *short* ($l = 5$) and the *long* ($l = 60$) scales in distinguishing the HP variability of healthy from those of heart disease patients.

Since the sign of ΔS captures the existing trends in the durations of the studied intervals through p_k, as mentioned (and not through their increments as in ref. [38]), we expect that novel dynamical features may be revealed if instead of δS_l the standard deviation $\sigma(\Delta S_l)$ of the time series of $\Delta S_l \equiv S_l - (S_-)_l$ is used. Thus, here we focus on the application of the complexity measures

$$\Lambda_l = \frac{\sigma(\Delta S_l)}{\sigma(\Delta S_3)}, \tag{3}$$

when a moving window of l heartbeats is sliding through the NN interval time series (cf. the latter intervals are [46] the beat to beat intervals which are obtained from consecutive pairs of normal beats, while intervals surrounding an ectopic beat are discarded, see also below). This complexity measure quantifies how the statistics of ΔS_l time series changes upon increasing the scale from 3 heartbeats to l heartbeats. If we recall that for randomly shuffled data $\sigma[\Delta S_{l,shuff}]$ is proportional [12] to the ratio of the standard deviation over the mean value of the data themselves (see eq.(3.78) of ref. [3]), we can see that Λ_l being a ratio of $\sigma(\Delta S_l)$ between different scales is expected to be independent of σ/μ and hence it may reveal information hidden in the original NN intervals time series.

Data and Analysis. – The data analyzed come from 134 long-lasting (from several hours to around 24 h) ECG recordings available from databases [47] containing: (i) 72 healthy (H) subjects (i.e., the MIT-BIH Normal Sinus Rhythm Database (nsrdb) containing 18 H and the Normal Sinus Rhythm RR Interval Database (nsr2db) containing 54 H, both digitized with frequency f_{exp}=128Hz), (ii) 44 patients with CHF (i.e., the Congestive Heart Failure RR Interval Database (chf2db) containing 29 subjects with f_{exp}=128Hz and the BIDMC Congestive Heart Failure Database (chfdb) with 15 subjects with severe congestive heart failure which is subset of the data described in ref. [48], f_{exp}=250Hz), and (iii) the Sudden Cardiac Death Holter Database (sddb) digitized with f_{exp}=250Hz. The latter contains 24 individuals among which 12 had ECG with audited annotations. Here, beyond these 12 individuals, we studied six more (i.e., "33", "37", "44", "47", "48", "50") whose ECG could be analyzed with confidence as reported in ref. [12]. Thus, we consider 18 (out of 24) SCD individuals of the sddb.

The present results refer, as mentioned, to the NN intervals, i.e., Q_k=NN$_k$. These intervals were obtained [49] from the ECG annotation files by using the option '-c -PN -pN', and following ref. [28], we eliminate d outliers due to missed beat detections that may give rise to large intervals included in the NN time series.

Each of the 134 NN time series was analyzed in natural time by using a moving window of length l heartbeats sliding through the NN time series. For each position of the moving window, we obtained through eqs.(1) and (2) S and S_- and therefrom the ΔS_l time series which is highly fluctuating. For the quantification of these fluctuations, its standard deviation $\sigma[\Delta S_l]$ was estimated for $l = 3, 4, \ldots, 100$. These values are stable since the number of samples -analyzed intervals- is usually much larger than 10^4. Finally, using eq.(3) we evaluated the complexity measures Λ_l.

Results. – Figure 2 depicts the mean value of Λ_l together with the standard error of the mean for the three classes H, CHF and SCD. We observe that the healthy class H exhibits the highest values of Λ_l in accordance with the already mentioned observations of highest complexity in healthy heart dynamics , while SCD class the lower bound. The congestive heart failure class CHF lies in between H and SCD, being closer to SCD for small scales l and approaching H for the larger scales. This prompted us to investigate how the possible discrimination between the three classes is affected upon changing l.

By assigning a heart malfunction index M which takes the value $M = 0$ for H, $M = 0.5$ for CHF and $M = 1.0$ for SCD, we used the Receiver Operating Characteristics (ROC) method [50] to separate between the three classes. ROC is a method to evaluate binary predictions based on a graph depicting the hit rate h (or sensitivity) versus the false alarm rate f (cf. for the specificity, usually used in medical context [51], the relation specificity=1-f holds). We first select a threshold M_c and if $M \geq M_c$ we have a positive individual (a patient in our case), otherwise the individual is considered negative. We then examine whether the corresponding complexity measure Λ_l lies below a given threshold $[\Lambda_l]_c$: if $\Lambda_l \leq [\Lambda_l]_c$ then we assign to this individual a "positive" hypothesized class otherwise a "negative" hypothesized class is assigned. The hit rate h is the ratio of the number of positive individuals belonging to the "positive" hypothesized class over the total number of positive individuals. The false alarm rate f is the ratio of the number of negative individuals belonging to the "positive" hypothesized class over the total number of negative individuals. The ROC curve, see fig.3, is the plot of h versus f which is obtained when we vary the threshold $[\Lambda_l]_c$. A random predictor yields ROC curves around the diagonal and the statistical significance of a predictor can be estimated [52] by evaluating the area under the curve (AUC) in the ROC diagram (see also ref. [53]). When the number of positive and negative individuals remains the same (as holds here), the larger AUC signifies a smaller probability to obtain the results by chance, and hence a higher statistical significance.

Figure 4 depicts the AUCs obtained versus the scale l used for the estimation of Λ_l for the two thresholds $M_c = 0.5$ (red pluses) and $M_c = 1.0$ (green crosses), i.e., when attempting to distinguish both CHF and SCD from H as well as attempting to distinguish SCD from H and CHF, respectively. We observe that in the former case, AUC maximizes at small scales ($l = 7$) whereas in the latter case a broad maximum appears between $l = 40$ to $l = 70$ where AUC reaches its largest value at $l = 49$. Thus, two optimum scales $l = 7$ and $l = 49$ appear.

Figures 3(a) and 3(b) show the corresponding ROC curves for $M_c = 0.5$ and $M_c = 1.0$, respectively. In each case, the colored contours depict the probability p to obtain by chance an ROC point in the ROC diagram as it results [53] from the study of confidence ellipses. This visualization scheme for the statistical significance of ROC curves is based [53] on the k-ellipses which are the envelop es of the confidence ellipses -cf. a point lies outside a confidence ellipse with probability exp(−k/2)- obtained when using a random predictor and vary the prediction threshold. The k-ellipses cover the whole ROC plane and using their AUC we can have a measure [53] of the probability p to obtain by chance (i.e., using a random predictor) an ROC curve passing through each point on the ROC plane. We observe that in both cases highly statistically significant results are obtained that lie well above the $p = 1\%$ k-ellipses.

We now turn to the problem of classifying the three different classes H, CHF and SCD. For this reason, we propose the use of ROC diagrams depicted in figs.3(a) and 3(b) in the following two steps: In the first step, we shall try to discern the healthy group from both CHF and SCD. Hence, we are interested in the results obtained when using $M_c = 0.5$. The corresponding AUCs are depicted with the (red) crosses in fig. 4 and stress the importance of the scale $l = 7$. Thus, using fig.3(a) we focus in the ROC region with false alarm rate $f < 0.1$, and hence efficiency larger than 90%. The results show that when using the value $[\Lambda_7]_c$=1.97 we can obtain a hit rate $h \approx 66\%$ with $f \approx 8\%$. In the second step, we focus on the discrimination of SCD from both H and CHF. In this case, the optimum scale, found on the basis of fig.4, is $l = 49$ and a study of the results depicted in fig.3(b) reveals that when using the value $[\Lambda_{49}]_c$=2.07 a hit rate $h \approx 67\%$ is reached with a false alarm rate of only $f \approx 3\%$. Figure 5 depicts the complexity measure Λ_{49} versus Λ_7 for all the individuals studied. We observe that when using the aforementioned thresholds $[\Lambda_7]_c$ and $[\Lambda_{49}]_c$, depicted in fig.5 by the (blue) vertical and the (red) horizontal line respectively, the vast majority of SCD populates the bottom part, whereas most of CHF and H lie in the left and the right side of the upper part. Especially, for H only 5 out of the 72 individuals studied mix with CHF. The sensitivity s in each of the three regions defined in fig.5 is the

following: for the H region, i.e., when $\Lambda_7 > [\Lambda_7]_c$ and $\Lambda_{49} > [\Lambda_{49}]_c$, we have $s_H = 93\%$, for the CHF region, i.e., when $\Lambda_7 < [\Lambda_7]_c$ and $\Lambda_{49} > [\Lambda_{49}]_c$, we obtain $s_{CHF} = 57\%$ and for the SCD ($\Lambda_{49} < [\Lambda_{49}]_c$) $s_{SCD} = 67\%$. It is remarkable that only 4 SCD individuals mix with H and that this number may become smaller if we use the complementarity of the present complexity measures with those already defined in natural time to which we turn in the next Section.

Discussion. – In ref. [12], the complexity measure $N_3 \equiv \sigma[\Delta S_{3,shuff}]/\sigma[\Delta S_3]$ together with $\sigma[\Delta S_7]$ have been used for the discrimination of SCD from H and CHF. The results (see fig.3(a) of ref. [12]) showed that only the SCD individuals labeled "32" and "41" mixed with CHF whereas "30" and "49" mixed with H. Interestingly, from these individuals only "49" mixes with H in fig.5. Moreover, in the present analysis "30" and "32" are the two SCD which mix in fig.5 with the CHF and "41" lies in the region of SCD. This points to the fact that the complexity measures Λ_l are, as already mentioned, complementary to those used in ref. [12]. Λ_l are also complementary to standard, largely utilized, time domain linear parameters like SDNN used for the separation of CHF from H. For example, when we consider SDNN (resulting to AUC=0.848 for $M_c = 0.5$ and AUC=0.532 for $M_c = 1.0$, i.e., definitely smaller than those for l=7 and 49 in fig.4) 10 CHF -as well as 9 SCD- mix with H (moreover 7 SCD mix with CHF) but only 7 of these mixed CHF individuals appear in the region of H in fig.5. Moreover, when comparing the remaining two SCD which do not mix with H and CHF, we find that one of them ("33") lies in the region of H in fig.5. For the differentiation of H from CHF, a largely utilized complexity measure is the sample entropy [54]. We evaluated it by making use of the computer code `sampen` [55] (for m=2 and r=0.2) and found that only 12 CHF do not mix with H and the latter are also mixed with 10 SCD (giving rise to AUCs, for both M_c's considered, smaller than 0.65). On the other hand, 6 SCD can be clearly distinguished from both H and CHF. Among these 6 SCD there are three cases ("33", "34" and "47") which appear in the region of H in fig.5. In other words, if we compare the results of fig.5 with those of `sampen`, only one SCD ("49") remains in the region of H. Interestingly, this result is similar to that found above when comparing fig.5 with fig.3(a) of ref. [12].

Now concerning the separation of CHF from the other two classes, we have to recall that in ref. [12] $\sigma[\Delta S_7]$ has been proven to be useful in this direction and the majority of CHF exhibited $\sigma[\Delta S_7]$ smaller than a threshold $\{\sigma[\Delta S_7]\}_c = 0.00052$. If we apply this additional condition in the region labeled H in fig.5, we find that 5 CHF individuals can be excluded from this region lea ving only 11 CHF mixed with H. The results of the application of such a three dimensional selection scheme based on Λ_7, Λ_{49}, and $\sigma[\Delta S_7]$ leads to the contingency table presented in table 1. An inspection of this table shows that in all three cases H, CHF and SCD there exists a probability $\approx 80\%$ for an individual belonging to a given hypothesized class to truly come from this class. Additionally, we investigated the selection of the normalization factor $\sigma(\Delta S_3)$ in eq.(3) as a possibility to obtain a better discrimination between H, CHF and SCD. To this end, the present analysis was repeated by considering $\sigma(\Delta S_\nu), \nu = 4, 5, \ldots 100$, instead of $\sigma(\Delta S_3)$ in the denominator of eq.(3). The results showed that only the selection $\nu = 4$ exhibits a slightly higher (0.00675 on average) maximum AUC, see the lines labeled (1) and (2) in fig. 4, than those obtained when using Λ_l of eq.(3). The optimum scales selected on the basis of these AUCs are $l' = 5$ for $M_c = 0.5$ and $l' = 55$ for $M_c = 1.0$ which do not differ essentially from $l = 7$ and 49. We further proceeded as in the case of Λ_l by defining critical values similar to $[\Lambda_7]_c$ and $[\Lambda_{49}]_c$ exhibiting efficiency larger than 90%, and finally constructed the (corresponding to table 1) contigency table when also using $\sigma[\Delta S_7]$. The only differences found were that 10 CHF belonged to the "h" hypothesized class and 4 CHF to the "scd" hypothesized class, instead of 11 and 3 respectively in table 1. The additional results of fig.4, however, indicate that $\nu = 3$ or 4 are the appropriate scales for the normalization factor in eq.(3) so that AUC is maximized. This result compares favorably with those of ref. [56], which revealed that the most likely

length of the most informative patterns in HP variability ranges from 2 to 4.

Let us now discuss on the physical meaning behind the selection of Λ_7 and Λ_{49} that have been found on the basis of fig.4 to exhibit an optimum discrimination between H, CHF and SCD. Λ_l quantifies, as mentioned, the change in the statistics of ΔS_l upon changing the scale from 3 to l. Thus, three important scales emerge from the present analysis which are $l = 3$, 7, and 49. These three scales are closely related to the spectral density study of heart rate variability [46]. A variety of research has established [57], two clear frequency bands in heart rate and blood pressure with autonomic involvement: (i) A higher frequency (HF) band, which lies in [58, 59] the range 0.15 to 0.40Hz and is [31] "indicative of the presence of respiratory modulation of the heart rate" or reflects [58] "modulation of vagal activity, primarily by breathing" (ii) A lower frequency (LF) band from 0.04 to 0.15Hz (i.e., at around 0.1Hz) which is usually described as corresponding to [59] "the process of slow regulation of blood pressure and heart rate" or that [58] "it reflects modulation of sympathetic or parasympathetic activity by baroflex mechanisms" due to [31] "the emergence of a limit cycle caused by the vascular sympathetic delay" (cf. its exact explanation, however, is still strongly debated [60]). Moreover, the existence of a very low frequency band (VLF) in the region 0.003 to 0.04Hz has been identified [46]. The aforementioned scale $l = 3$ corresponds to HF whereas the scales $l = 7$ and $l = 49$ lie near to the transition from the HF to the LF band and from the LF band to the VLF band, respectively. Hence, the present results may be considered as extending those obtained in ref. [12] for the importance of the HF and LF band in distinguishing SCD from H by strengthening also the spectral part of the transition region from LF to VLF.

Conclusions. – The application of a new complexity measure Λ_l to the study of NN intervals in ECG has been investigated. Λ_l is the ratio of the standard deviations of the time series of the change of the entropy in natural time under time reversal obtained upon increasing the scale l from 3 to l heartbeats. The results obtained by means of the ROC method and Λ_l show that they are complementary to those obtained using other complexity measures in natural time. Using this complementarity, regions in the complexity measure space can be defined that lead to probabilities of $\approx 80\%$ to correctly identify an individual among the healthy, the congestive heart failure and sudden cardiac death groups. The physical interpretation of the results points to the importance of both limits of the LF band in HP variability when they are measured comparatively to the HF band.

REFERENCES

[1] Varotsos P. A., Sarlis N. V. and Skordas E. S., *Practica of Athens Academy*, **76** (2001) 294.
[2] Varotsos P. A., Sarlis N. V. and Skordas E. S., *Phys. Rev. E*, **66** (2002) 011902.
[3] Varotsos P. A., Sarlis N. V. and Skordas E. S., *Natural Time Analysis: The new view of time.* (Springer-Verlag, Berlin Heidelberg) 2011.
[4] Abe S. *et al.*, *Phys. Rev. Lett.*, **94** (2005) 170601.
[5] Varotsos P. A., Sarlis N. V. and Skordas E. S., *Phys. Rev. E*, **68** (2003) 031106.
[6] Varotsos P. A. *et al.*, *Phys. Rev. E*, **70** (2004) 011106.
[7] Varotsos P. A. *et al.*, *Phys. Rev. E*, **71** (2005) 032102.
[8] Lesche B., *J. Stat. Phys.*, **27** (1982) 419.
[9] Lesche B., *Phys. Rev. E*, **70** (2004) 017102.
[10] Varotsos P. A., Sarlis N. V. and Skordas E. S., *Phys. Rev. E*, **67** (2003) 021109.
[11] Varotsos P. A., Sarlis N. V. and Skordas E. S., *CHAOS*, **19** (2009) 023114.
[12] Varotsos P. A. *et al.*, *Appl. Phys. Lett.*, **91** (2007) 064106.
[13] Varotsos P. A. *et al.*, *J. Appl. Phys.*, **103** (2008) 014906.
[14] Sarlis N., Skordas E. and Varotsos P., *Tectonophysics*, **513** (2011) 49.
[15] Olami Z., Feder H. J. S. and Christensen K., *Phys. Rev. Lett.*, **68** (1992) 1244.
[16] Varotsos C. and Tzanis C., *Atmos. Environ.*, **47** (2012) 428.

[17] Varotsos C. and Tzanis C., *Atmos. Chem. Phys. Discuss.*, **12** (2012) 17443.
[18] Sarlis N. V., Skordas E. S. and Varotsos P. A., *EPL*, **87** (2009) 18003.
[19] Goldberger A. L. *et al.*, *Proc. Natl. Acad. Sci. USA*, **99** (2002) 2466.
[20] Ho K. *et al.*, *Circulation*, **96** (1997) 842.
[21] Pikkujämsä S. *et al.*, *Circulation*, **100** (1999) 393.
[22] Zorick T. and Mandelkern M. A., *PLoS ONE*, **8** (2013) e68360.
[23] Peng C.-K. *et al.*, *Phys. Rev. Lett.*, **70** (1993) 1343.
[24] Peng C.-K. *et al.*, *CHAOS*, **5** (1995) 82.
[25] Havlin S. *et al.*, *Physica A*, **273** (1999) 46.
[26] Ashkenazy Y. *et al.*, *Comput. Cardiol.*, **27** (2000) 139.
[27] Ashkenazy Y. *et al.*, *Phys. Rev. Lett.*, **86** (2001) 1900.
[28] Ivanov P. C. *et al.*, *Nature*, **399** (1999) 461.
[29] Ivanov P. C. *et al.*, *CHAOS*, **11** (2001) 641.
[30] Ivanov P. C. *et al.*, *Physica A*, **344** (2004) 685.
[31] Kotani K. *et al.*, *Phys. Rev. E*, **72** (2005) 041904.
[32] Reyes-Ramírez I. and Guzmán-Vargas L., *EPL*, **89** (2010) 38008.
[33] Makowiec D. *et al.*, *Physiological Measurement*, **32** (2011) 1681.
[34] Ashkenazy Y. *et al.*, *Europhys. Lett.*, **53** (2001) 709.
[35] Peng C.-K. *et al.*, *Phys. Rev. E*, **49** (1994) 1685.
[36] Ivanov P. C. *et al.*, *Europhys. Lett.*, **48** (1999) 594.
[37] Costa M., Goldberger A. L. and Peng C.-K., *Phys. Rev. Lett.*, **89** (2002) 068102.
[38] Costa M., Goldberger A. L. and Peng C.-K., *Phys. Rev. Lett.*, **95** (2005) 198102.
[39] Porta A. *et al.*, *Comp. Cardiol.*, **33** (2006) 77.
[40] Porta A. *et al.*, *Am. J. Physiol. - Regul. Integr. Comp. Physiol.*, **295** (2008) R550.
[41] Casali K. R. *et al.*, *Phys. Rev. E*, **77** (2008) 066204.
[42] Costa M., Peng C.-K. and Goldberger A., *Cardiovasc. Eng.*, **8** (2008) 88.
[43] Porta A. *et al.*, *Phil. Trans. R. Soc. A*, **367** (2009) 1359.
[44] Varotsos P. A. *et al.*, *Practica of Athens Academy*, **78** (2003) 281.
[45] Varotsos P. A. *et al.*, *Phys. Rev. E*, **71** (2005) 011110.
[46] Task force of the European Society of Cardiology and the North American Society of Pacing and Electrophysiology, *Circulation*, **93** (1996) 1043.
[47] Goldberger A. L. *et al.*, *Circulation*, **101** (2000) E215 (see also `www.physionet.org`).
[48] Baim D. S. *et al.*, *J. Am. Coll. Cardiol.*, **7** (1986) 661.
[49] Moody G. B., Computer code `ann2rr` of PhysioToolkit in Physionet available from `www.physionet.org/physiotools/wag/ann2rr-1.htm`.
[50] Fawcett T., *Pattern Recogn. Lett.*, **27** (2006) 861.
[51] Swets J., *Science*, **240** (1988) 1285.
[52] Mason S. J. and Graham N. E., *Quart. J. Roy. Meteor. Soc.*, **128** (2002) 2145.
[53] Sarlis N. V. and Christopoulos S.-R. G., *Comput. Phys. Commun.*, **185** (2014) 1172.
[54] Richman J. S. and Moorman J. R., *Am. J. Physiol. Heart Circ. Physiol.*, **278** (2000) H2039.
[55] Lake D. K., Moorman J. R. and Hanqing C., *Computer code* `sampen` *available from* `http://www.physionet.org/physiotools/sampen/`, (2004) .
[56] Porta A. *et al.*, *CHAOS*, **17** (2007) 015117.
[57] Malpas S. C., *Am. J. Physiol. Heart. Circ. Physiol.*, **282** (2002) H6.
[58] Bigger J. T. Jr. *et al.*, *Circulation*, **91** (1995) 1936.
[59] Prokhorov M. D. *et al.*, *Phys. Rev. E*, **68** (2003) 041913.
[60] McSharry P. E. *et al.*, *IEEE Trans. Biomed. Eng.*, **550** (2003) 289.

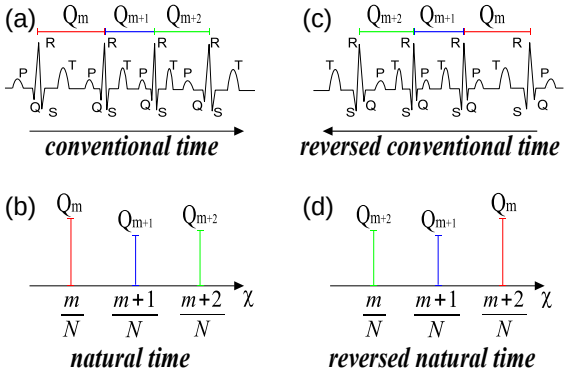

Fig. 1: (color online) How an ECG in conventional time (a) is read in natural time (b) when Q_k =RR$_k$. Panels (c) and (d) correspond to (a) and (b), respectively, under time reversal.

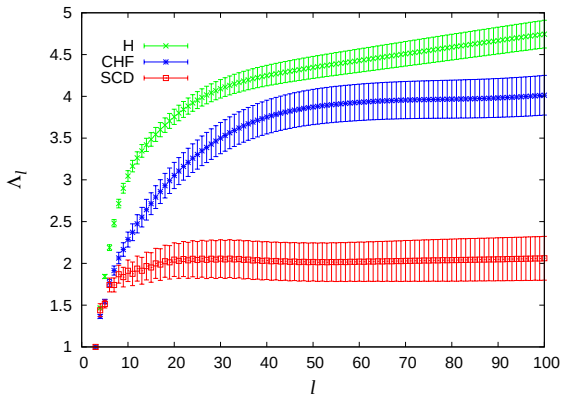

Fig. 2: (color online) The complexity measure Λ_l vs the scale l for the three classes H, CHF and SCD. The mean value for each scale and class together with the standard error are shown.

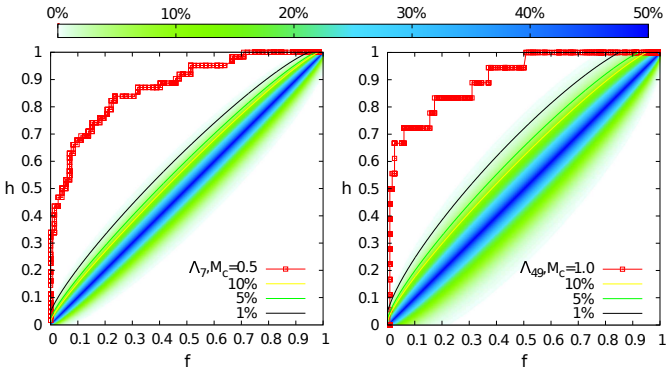

Fig. 3: (color online) Receiver Operating Characteristics (red squares) when using Λ_l as a predictor: (a) for $l = 7$ with M_c=0.5 and (b) for $l = 49$ with $M_c = 1.0$. The colored contours depict [53] the probability p to obtain by chance an ROC point. The k-ellipses with p =10%, 5% and 1% are also drawn.

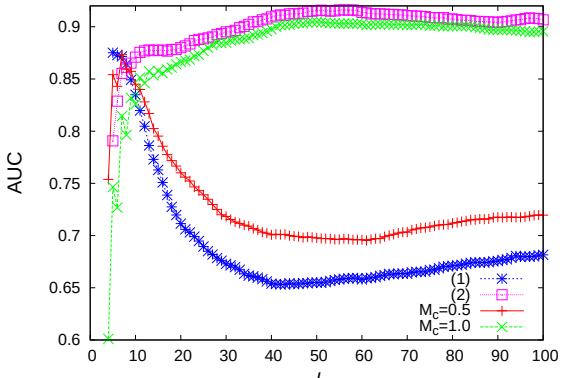

Fig. 4: (color online) The area under the ROC curve, AUC, when using Λ_l as a predictor for M_c=0.5 (red pluses) and M_c=1.0 (green crosses). The lines labeled (1) (blue asterisks) and (2) (magenta squares) correspond to M_c=0.5 and M_c=1.0, respectively, when using $\sigma(\Delta S_4)$ instead of $\sigma(\Delta S_3)$ in the denominator of eq.(3).

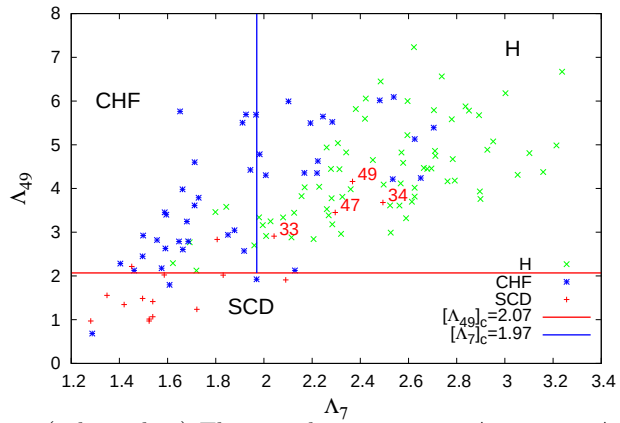

Fig. 5: (color online) The complexity measure Λ_{49} versus Λ_7 for all the individuals studied. The (red) horizontal line corresponds to $[\Lambda_{49}]_c = 2.07$, while the vertical (blue) one to $[\Lambda_7]_c = 1.97$. The labels of SCD that mix with H are also shown.

Table 1: Contingency table when using Λ_7, Λ_{49}, and $\sigma[\Delta S_7]$ for the attribution of the 134 individuals studied in the hypothesized classes "h", "chf" and "scd". An individual is hypothesized: "scd" if its Λ_{49} is smaller than $[\Lambda_{49}]_c$, "h" if its Λ_7, Λ_{49} and $\sigma[\Delta S_7]$ are larger than the corresponding thresholds mentioned in the text, and "chf" otherwise.

	H	CHF	SCD	
"h"	66	11	4	81
"chf"	6	30	2	38
"scd"	0	3	12	15
	72	44	18	134